Venkatasamy *et al.*
Acta Neuropathologica Communications (2025) 13:90
https://doi.org/10.1186/s40478-025-01998-x

Acta Neuropathologica Communications

RESEARCH

Open Access

Systemic IGF-1 administration prevents traumatic brain injury induced gut permeability, dysmorphia, dysbiosis, and the increased number of immature dentate granule cells

Lavanya Venkatasamy[1†], Jaclyn Iannucci[1†], Aleksandr Pereverzev[1†], Jonathan Hoar[1], Emily Huber[1], Angel Ifegbo[1], Reagan Dominy[1], Yumna El-Hakim[1], Kathiresh Kumar Mani[1], Alan Dabney[2], Rachel Pilla[3], Farida Sohrabji[1] and Lee A. Shapiro[1*]

Abstract

Traumatic brain injury (TBI) occurs in 2–3 million Americans each year and is a leading cause of death and disability. Among the many physiological consequences of TBI, the hypothalamic pituitary axis (HPA) is particularly vulnerable, including a reduction in growth hormone (GH) and insulin-like growth factor (IGF-1). Clinical and preclinical supplementation of IGF-1 after TBI has exhibited beneficial effects. IGF-1 receptors are prominently observed in many tissues, including in the brain and in the gastrointestinal (GI) system. In addition to causing damage in the brain, TBI also induces GI system damage, including inflammation and alterations to intestinal permeability and the gut microbiome. The goal of this study was to assess the effects of systemic IGF-1 treatment in a rat model of TBI on GI outcomes. Because GI dysfunction has been linked to hippocampal dysfunction, we also examined proliferation and immature granule cells in the hippocampal dentate gyrus. 10-week-old male rats were treated with an intraperitoneal (i.p.) dose of IGF-1 at 4 and 24 h after lateral fluid percussion injury (FPI). At 3- and 35-days post-injury (DPI), gut permeability, gut dysmorphia, the fecal microbiome, and the hippocampus were assessed. FPI-induced permeability of the blood-gut-barrier, as measured by elevated gut metabolites in the blood, and this was prevented by the IGF-1 treatment. Gut dysmorphia and alterations to the microbiome were also observed after FPI and these effects were ameliorated by IGF-1, as was the increase in immature granule cells in the hippocampus. These findings suggest that IGF-1 can target gut dysfunction and damage after TBI, in addition to its role in influencing adult hippocampal neurogenesis.

Keywords TBI, Gut microbiome, Gastrointestinal system, Fluid percussion injury (FPI), Hippocampus, Metabolite, Neurogenesis, Dentate gyrus, Newborn neurons, Growth hormone

†Lavanya Venkatasamy, Jaclyn Iannucci, and Aleksandr Pereverzev have contributed equally to this work.

*Correspondence:
Lee A. Shapiro
lshapiro@tamu.edu
Full list of author information is available at the end of the article

Background

Traumatic brain injury (TBI) occurs in 2–3 million Americans each year, and as many as 50 million people worldwide [1, 2]. TBI is a leading cause of death and disability [3, 4], and suffering a TBI is associated with an approximately 2.2–2.8-fold increase in 30-year mortality rate [5]. TBI is also associated with a number of chronic post-traumatic syndromes, including depression, cognitive impairment, and an increased susceptibility to chronic neurodegenerative disorders, such as post-traumatic epilepsy, Parkinson's disease (PD), and Alzheimer's disease (AD) [3, 6]. There are currently no effective treatments for mitigating post-traumatic syndromes, and identifying therapeutic mechanisms is of the utmost importance to improve health outcomes for the millions of people who experience a TBI each year, and are living with the consequences [5].

Among the myriad of physiological consequences to a TBI, the hypothalamic–pituitary–adrenal axis (HPA) is particularly vulnerable. The HPA regulates hormonal release and endocrine function, and HPA dysregulation after TBI has been identified in clinical [7–13] and preclinical studies [14–16]. This pathology can manifest as abnormal hormone production [17–20], including disruption in growth hormone (GH) released from the pituitary gland [21–23] and reduced insulin-like growth factor-1 (IGF-1) that is primarily released by the liver in response to endocrine signals. Importantly, these physiological consequences may play a role in TBI pathogenesis [10, 24, 25], and in a Phase II clinical trial, supplementing IGF-1 after TBI alone, or in combination with GH, improved weight gain, nutritional status, and other metabolic parameters in moderate-to-severe TBI patients in the first two weeks after injury [26–28].

IGF-1 is a 7.5 kDa peptide hormone that plays a major role in cell growth, differentiation, and repair, including after central nervous system (CNS) trauma [29–34]. Reduced serum IGF-1 has been reported in patients during the first week after TBI [35, 36] and more chronically after injury [37, 38]. Reduced levels of IGF binding proteins (IGFBP), which bind to and stabilize IGF-1 for transport in the serum, have also been identified after TBI [39]. Interestingly, higher levels of serum IGF-1 after TBI was predictive of white matter recovery and memory improvement after injury [40], and low serum IGF-1 in children was associated with worse outcomes [41].

Preclinical TBI studies also demonstrate reduced IGF-1 after TBI. Following TBI in adolescent rats, serum IGF-1 was decreased between 1 week and 1 month after injury [42], and this reduction was correlated with impaired cognitive function [43]. In another study, plasma IGF-1 was reduced 3 weeks after controlled cortical impact (CCI) in mice [44]. Thus, IGF-1 deficiency after clinical and preclinical TBI appears to be associated with detrimental neuropathological outcomes. Accordingly, IGF-1 treatment for 14 days elevated serum IGF-1, and the elevations were associated with increased survival and a higher percentage of patients achieving better outcome scores 6 months after injury [26], and this is supported by preclinical studies [45–47]. While side effects such as hypoglycemia may limit the therapeutic potential of IGF-1 [48], identification of novel targets could enable studies to overcome this limitation.

After TBI, exogenous IGF-1 may convey benefit in the periphery, as well as in the CNS. In the periphery, the gastrointestinal (GI) tract is damaged after TBI, including altered intestinal permeability [49–51], inflammation [51, 52], and alterations to the microbiome [52–61]. IGF-1 receptors are prominently expressed in the gut where they are involved in regulating intestinal epithelial stem cell (IESC) function [62, 63]. The GI system is increasingly recognized as playing a major role in mediating neuropathology and neurological dysfunction, and IGF-1 may be involved in the GI response to injury [62, 64–70], including inflammation induced gut permeability [71, 72]. Importantly, gut dysfunction has been shown to worsen the neurological deficits associated with TBI [73]. Therefore, the present study investigated the hypothesis that systemic IGF-1 treatment at 4 and 24 h after FPI would improve GI permeability, dysmorphia, and alterations to gut microbiome. Because TBI is known to alter the number and morphology of immature dentate granule neurons [74–77], and because IGF-1 has been previously shown to alter hippocampal neurogenesis in the context of TBI [46], this study also examined immature neurons in the hippocampus after FPI.

Results

FPI-induced gut permeability at 3-days post-FPI is attenuated by IGF-1

GI permeability was assessed at 3 days post injury (DPI) by measuring serum levels of LPS, iFABP, and Mucin-2 (Muc-2), elevations of which are indicative of increased intestinal permeability and gut barrier damage [78–80]. LPS is an endotoxin released by Gram-negative bacteria, and the concentration of LPS has been reported to be increased in plasma due to an impaired gut barrier after TBI [73, 81]. iFABP and muc-2 are major components of the mucosal layer, and they can be released into circulation when there is damage to the mucosal layer [82, 83]. There was a

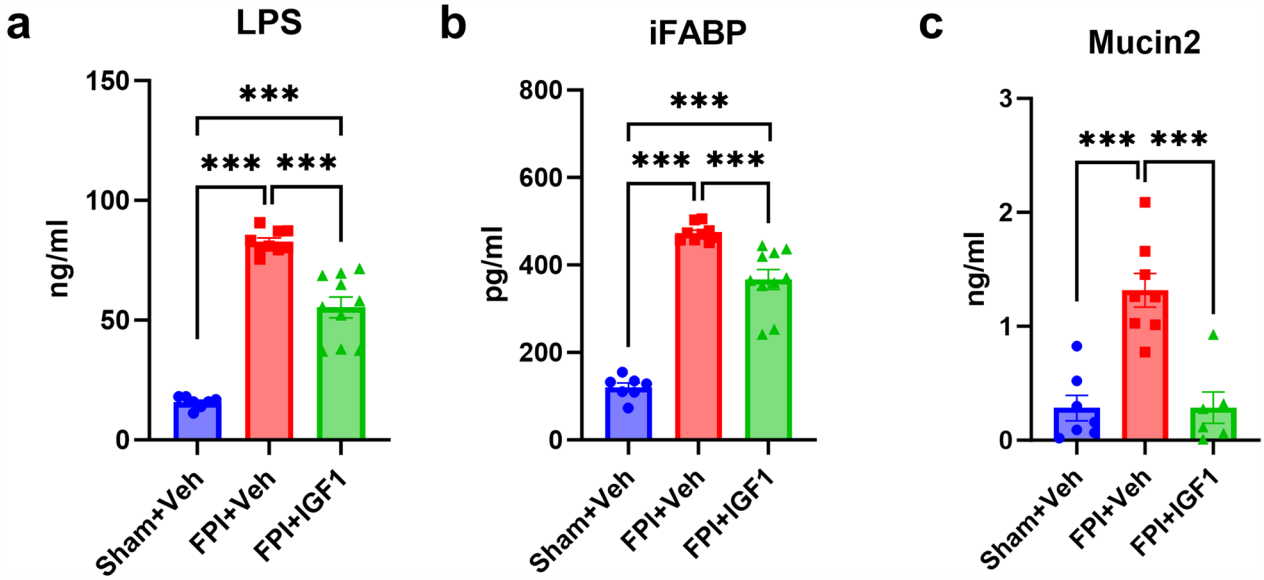

Fig. 1 IGF-1 treatment rescues early FPI-induced gut permeability. Blood-gut barrier permeability was assessed at 3 DPI by measuring serum levels of LPS, iFABP and Muc-2 [78–80]. In **a**, there was a significant increase in the serum concentration of LPS in the FPI + Veh rats ($p < 0.0001$ vs. Sham + Veh) that was significantly ameliorated by IGF-1 treatment ($p < 0.001$ vs. TBI + Veh). In **b**, levels of serum iFABP were significantly elevated in FPI + Veh as compared to the Sham + Veh rats ($p < 0.0001$), and this increase was significantly attenuated in the FPI + IGF-1 rats ($p < 0.001$ vs. FPI + Veh). In **c**, the concentration of Muc-2 (520 kD) was significantly elevated in FPI + Veh rats compared to the Sham + Veh rats ($p < 0.0001$) and reduced in FPI + IGF-1 rats ($p < 0.001$ vs. FPI + Veh). These data suggest that the blood-gut barrier and the mucus barrier may deteriorate after FPI and this is prevented by IGF-1. Data are represented as Mean ± SEM; n = 8–10 per group. Note, 3 rats in the FPI + IGF-1 group were omitted from Mucin-2 analysis due to limited serum availability. ***$p < 0.001$; ****$p < 0.0001$

significant increase in the serum concentrations of LPS ($p < 0.0001$), iFABP ($p < 0.0001$), and Muc-2 ($p < 0.0001$) in the FPI + Veh group compared to sham, all of which were significantly decreased to sham levels in the FPI + IGF1 group ($p < 0.0001$, $p < 0.001$, $p < 0.001$, respectively vs. FPI + Veh) (Fig. 1a–c). These data show intestinal barrier permeability after FPI, and this can be mitigated by IGF-1 treatment.

Gut dysmorphia after FPI is diminished by IGF-1

To assess gut morphology, the ileum and proximal colon were analyzed (Fig. 2, Supp. Fig. Q1) using H&E staining at 3 and 35 DPI. Qualitatively, at 3 and 35 DPI the intestines of the FPI + Veh rats exhibited clear disruption relative to sham rats, while the FPI + IGF-1 treated rats resembled the shams. In the FPI + Veh rats, there appeared to be fewer villi in the ileum, and many of the villi appeared short and stubby, and this observation was more pronounced at 35 DPI. (Fig. 2a–f, k–p). Quantitative analysis of the villus length:width ratio and the number of crypts per villus were consistent with the qualitative observations. No significant differences in the ileum were observed at 3 DPI the villus (Fig. 2g, h), but at 35 DPI, FPI significantly reduced the length:width ratio of the ileum villi ($p < 0.05$) and significantly increased the number of crypts per villus ($p < 0.05$), compared to sham rats (Fig. 2o, p). Compared to FPI + Veh, IGF-1 treatment after FPI resulted in a significant increase in the length:width ratio ($p < 0.05$), and a significant decrease in the number of crypts per villus ($p < 0.05$), such that the appearance was very similar to the Sham + Veh rats (Fig. 2o, p). The average lengths and widths of the villi are also provided (Table 1). Similar to the ileum, in the proximal colon there were no significant differences identified at 3 DPI (Supp. Fig. 1a,b), but at 35 DPI, FPI significantly reduced inter-crypt mucosal length:width ratio ($p < 0.01$) and increased the number of crypts per inter-crypt mucosa ($p < 0.01$). As with the ileum, IGF-1 significantly prevented this FPI-induced gut dysmorphia, such that they appeared more like shams ($p < 0.01$, $p < 0.01$, respectively) (Supp. Fig. 1c, d).

Goblet cells in the gut epithelium produce the intestinal mucus, of which muc-2 is a major structural component [83, 84]. Quantitative analysis of the number goblet cells from PAS-stained tissue in the ileum at 3 and 35 DPI (Fig. 3a–c) revealed that FPI caused a significant decrease in the number of goblet cells at 3 DPI ($p < 0.05$ vs. Sham + Veh), and this was ameliorated by the IGF-1

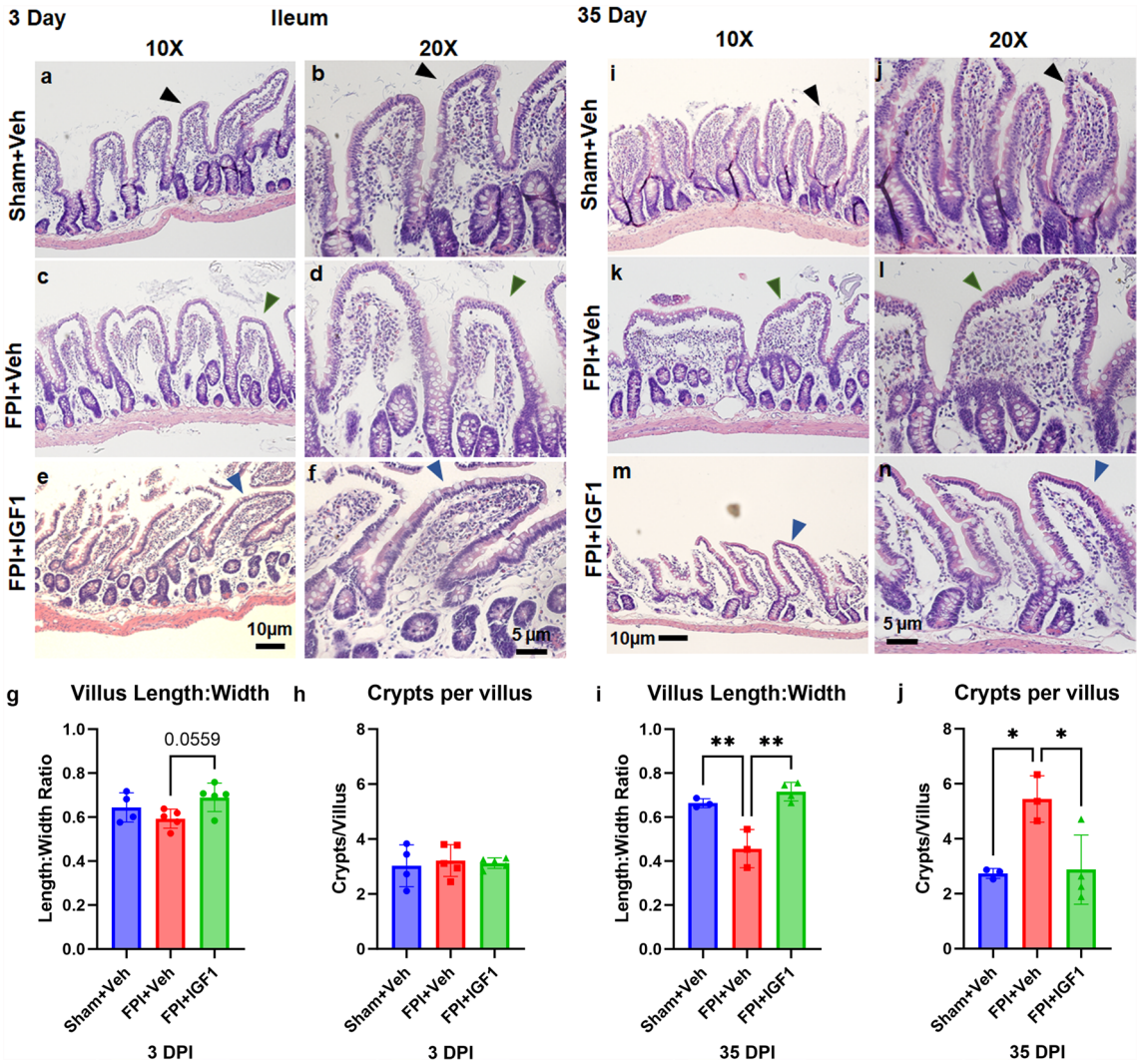

Fig. 2 IGF-1 treatment reduces FPI-induced chronic gut dysmorphia. To assess gut morphology, villi and crypts were analyzed in the ileum using H&E staining at 3 (**a**–**f**) and 35 (**j**–**o**) DPI. Note the normal appearance of the villi and crypts in sham rats (black arrowhead; a,b). Also note that at the 3 DPI timepoint, the villi are beginning to show a rounded stumpy appearance (green arrowhead; c,d), but the quantitative results are not significant at this time point (**g**, **h**). These morphological differences evolve over time so that they appear more pronounced at 35 DPI, such that they have a significantly reduced length:width ratio ($p < 0.01$ vs. Sham + Veh), and this was significantly increased by IGF-1 treatment ($p < 0.01$) (**o**). Importantly, the villi from the IGF-1 treated rats appears much more sham-like (e,f). In p, the number of crypts per villus in the ileum was increased after FPI ($p < 0.05$ vs. Sham + Veh), and IGF-1 treatment after FPI significantly reduced this effect ($p < 0.05$). For all rats, 3 slides were assessed, with 3 sections per slide measured. Scale bar in e,n = 10 μm for A,C,E,J,L,N; scale bar in f,o = 5 μm for B,D,F,L,M,O. Data are represented as Mean ± SEM. N for 3 DPI: 4 Sham + Veh, 5 FPI + Veh, 5 FPI + IGF1. N for 35 DPI: 3 Sham + Veh, 3 FPI + Veh, 4 FPI + IGF1. *$p < 0.05$; **$p < 0.01$

treatment ($p < 0.01$ vs. FPI + Veh; Fig. 3d). At 35 DPI a significant increase in the number of goblet cells per crypt following IGF-1 treatment was also observed ($p < 0.05$ vs. Sham + Veh, $p < 0.01$ vs. FPI + Veh; Fig. 3e), suggesting an influence of IGF-1 on goblet cells and mucus production. To determine the influence of FPI on proliferating cells in the ileum, Ki67-labeled cells were quantified. (Fig. 3f–h). Although no significant differences were observed at 3 DPI, IGF-1 treatment after FPI did result in a significant decrease in Ki67 + cells in the ileum ($p < 0.01$ vs. Sham + Veh; Fig. 3i). At 35 DPI, a significant increase in Ki67 + cells was observed in FPI + Veh rats ($p < 0.05$ vs. Sham + Veh), and this was significantly reduced by IGF-1 treatment ($p < 0.05$ vs. FPI + Veh; Fig. 3j). These data suggest that IGF-1 may have a protective effect on the intestinal mucosa, specifically the goblet cells, whereas it had the opposite effect on progenitor cells in the crypt after FPI.

Table 1 Average villus length and width at 3 and 35 DPI

Villus Length			
Treatment group	**Sham + Veh**	**FPI + Veh**	**FPI + IGF1**
3 DPI	214.4 ± 43.32	164.1 ± 12.55	210.7 ± 11.79
35 DPI	203.4 ± 8.43	171.1 ± 23.80	222.0 ± 29.00
Villus width			
Treatment group	**Sham + Veh**	**FPI + Veh**	**FPI + IGF1**
3 DPI	116.0 ± 11.30	114.0 ± 23.34	98.03 ± 36.08
35 DPI	106.0 ± 10.98	204.4 ± 46.65	89.36 ± 15.94

H&E staining was used to assess gut dysmorphia in the ileum at 3 and 35 DPI, and villus length and width were measured in µm. Values are expressed as Mean ± SD

Influence of IGF-1 on immature neurons and proliferative cells in the hippocampus after FPI

Because of the known effects of IGF-1 on the hippocampus, including adult hippocampal neurogenesis [46], this study examined immature neurons and Ki67 cells in the hippocampus at 3 DPI. Consistent with previous studies indicating that FPI induces early increases in adult hippocampal neurogenesis [74, 85], the results show that FPI resulted in a strong trend towards an increased number of DCX-labeled immature neurons in the dentate gyrus ($p = 0.051$, NS). This increase was not observed in the IGF-1-treated FPI group (Fig. 4a–c). It is pertinent to note that increased neurogenesis after precipitating brain injuries can include aberrant growth and integration of the newborn neurons [77, 86], resulting in dysfunctional hippocampal circuitry [77]. Thus, it is possible that the increased number of immature neurons in the dentate gyrus might contribute to the impaired hippocampal-dependent cognitive dysfunction that has been reported after FPI [87]. Examination of proliferating Ki67 + cells at 3 DPI yielded no significant differences in the dentate gyrus (Fig. 4e–h). These results suggest that FPI might be enhancing immature neuron survival, or increasing the rate of neurogenesis, rather than increasing the number of progenitor cells in the hippocampus at this timepoint.

Altered gut microbiome composition after TBI is normalized by IGF-1 treatment

Gut microbiome alterations have been observed acutely and chronically in clinical [54, 57] and preclinical models [59] of TBI, and have been linked to cognitive dysfunction [88, 89]. Therefore, fecal samples were collected at pre- and at 35 DPI, and analyzed via 16S sequencing. Changes to the Firmicutes to Bacteroidetes ratio (F:B) is an indicator of gut health [90], and changes to the abundance of major phyla can shift the F:B ratio [54, 56]. Here, the F:B ratio was significantly increased in the IGF-1 treated rats compared to the FPI + Veh ($p < 0.05$) (Fig. 5a). Further examination of Bacteroidetes levels after injury revealed a trend towards decreased Bacteroidetes in FPI + Veh rats compared to Sham + Veh ($p = 0.057$, NS) and a significant increase in Bacteroidetes after IGF-1 treatment ($p < 0.05$ vs. FPI + Veh) (Fig. 5b**).** Importantly, variations in bacterial phyla such as Bacteroidetes and Firmicutes have been associated with cognitive dysfunction [91–96], and the results from the current study show that FPI increased the relative abundance of Bacteroidetes. While there were no significant changes in Firmicutes (Fig. 5c), Firmicutes includes *Lactobacillus* species that are probiotic. At the species level, the abundance of *Lactobacillus* was significantly decreased in the FPI + Veh rats 35 DPI compared to baseline ($p < 0.05$), while there was no difference identified in either the Sham + Veh or IGF-1 treated groups when compared to baseline (Fig. 5d). Furthermore, using the partial Least-Squares Discriminant Analysis (PLS-DA), a multivariate dimensionality-reduction, to assess the major phyla present, the FPI + IGF rats were found to cluster more closely with the Sham + Veh, while the FPI + Veh exhibited greater variability (Fig. 5e). Thus, FPI shifts the gut microbiome population, and IGF-1 mitigates these effects.

Discussion

The results from this study demonstrate early and chronic changes to gut permeability, morphology, and the fecal microbiome after FPI, and an increase in the number of immature dentate granule cells. Clinical and preclinical TBI studies have demonstrated alterations to gut structure, function, and microbiome composition [53–59, 97–105]. GI dysfunction has been linked to neurobehavioral impairment, neuropsychiatric conditions, and neurodegenerative disease [106], and

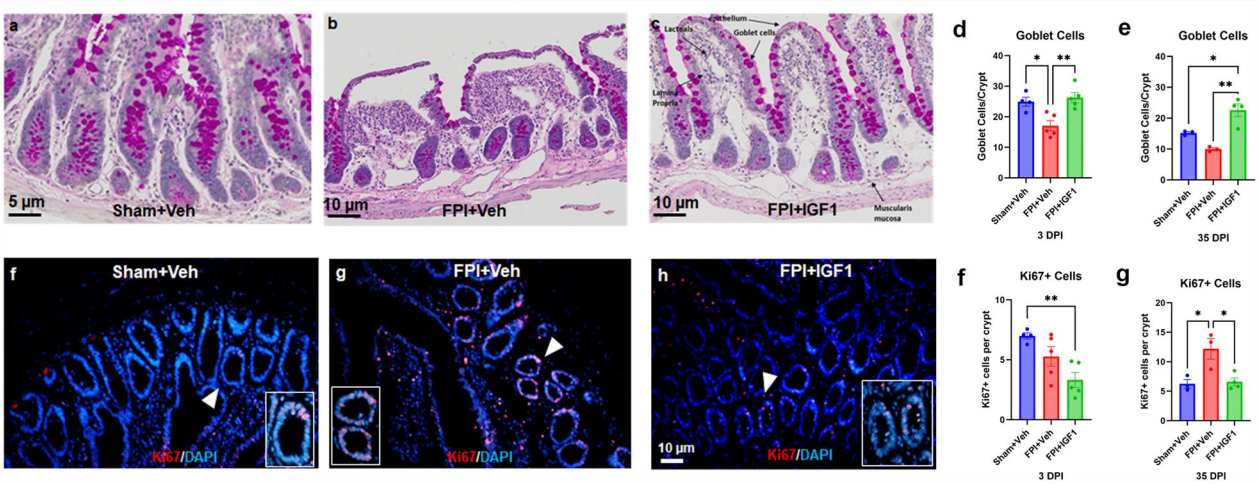

Fig. 3 Influence of FPI and IGF-1 on goblet cells and intestinal epithelial stem cells (IESC). PAS staining was used to assess the number of goblet cells per crypt in the ileum at 3 (**a**–**c**) and 35 DPI. Quantitative analysis revealed that FPI significantly reduced the number of goblet cells per crypt at 3 DPI (**d**) and 35 DPI (**e**) and this was increased by IGF-1 treatment. Proliferating IESCs in the crypts were determined by quantifying Ki67 + labeled cells at 3 (**i**) and 35 (**j**) DPI. In **f**–**h**, representative micrographs of Ki67 + staining in the crypts of the ileum at 35 DPI, with areas designated by the white arrow enlarged in the corresponding inset. At 3 DPI (**i**), the FPI + Veh showed a non-significant reduction ($p = 0.2152$, NS) in the number of Ki67 + cells in the crypts. The FPI + IGF-1 group exhibited a significant reduction ($p < 0.01$ vs. to Sham + Veh) in the Ki67 + cells in the crypts. Conversely at 35 DPI (**j**), FPI significantly increased the number of Ki67 + cells, and this was significantly reduced by IGF-1 treatment. This suggests that FPI resulted in a delayed increase in IESC proliferation, whereas IGF-1 reduced the number of Ki67 + cells at both timepoints examined. For all rats, 3 slides were assessed, with 3 sections per slide measured. Data are represented as Mean ± SEM; N for 3 DPI: 4 Sham + Veh, 5 FPI + Veh, 5 FPI + IGF1. N for 35 DPI: 3 Sham + Veh, 3 FPI + Veh, 4 FPI + IGF1. *$p < 0.05$; **$p < 0.01$. Scale bar in **a** = 5 µm; scale bar in **b,c** = 10 µm; scale bar in **h** = 10 µm for **f**–**h**

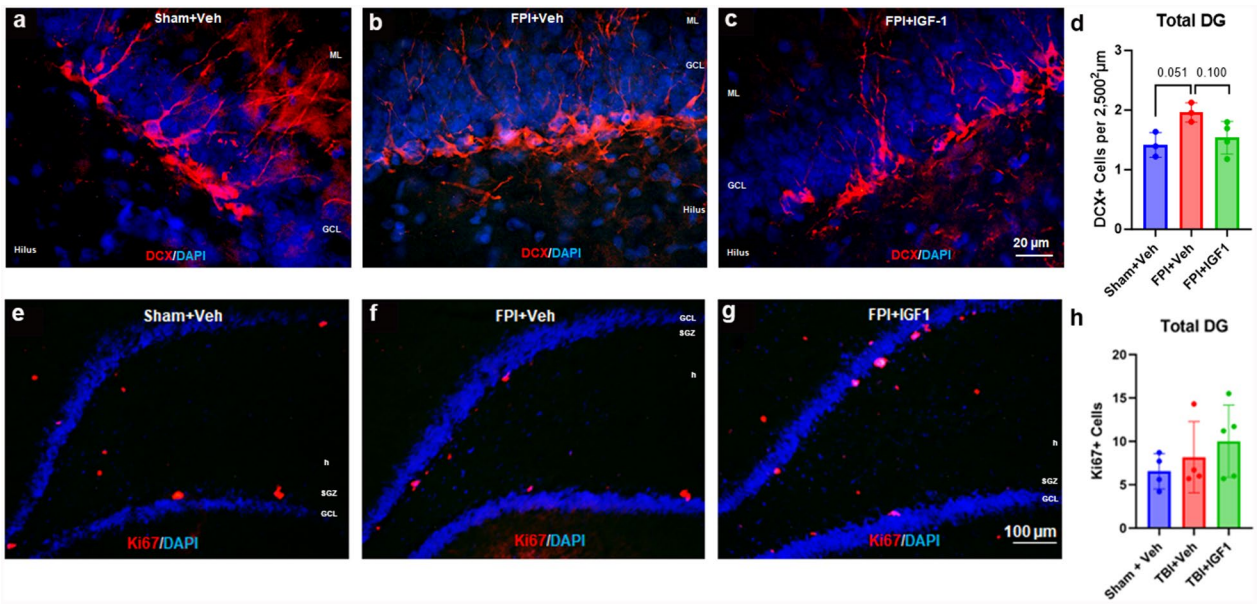

Fig. 4 IGF-1 ameliorates the FPI-induced increase in immature neurons in the adult hippocampus. Immature neurons in the hippocampal dentate gyrus were assessed by stereological quantification of the number of DCX-labeled cells at 3 DPI (**a**–**c**). The results show that FPI increased the number of DCX + cells ($p = 0.051$), and this was mitigated by IGF-1 treatment (**d**). The number of proliferative cells in the dentate gyrus (DG) was assessed by quantifying the number of Ki67-labeled cells (**e**–**g**) in the hilus (**h**), granule cell layer (GCL), and subgranular zone (SGZ). No significant differences in the number of Ki67 + cells in the hippocampus were identified at 3 DPI (**h**). Scale bar in c = 20 µm for (**a**–**c**). Data are represented as Mean ± SEM; n = 3–4 per group

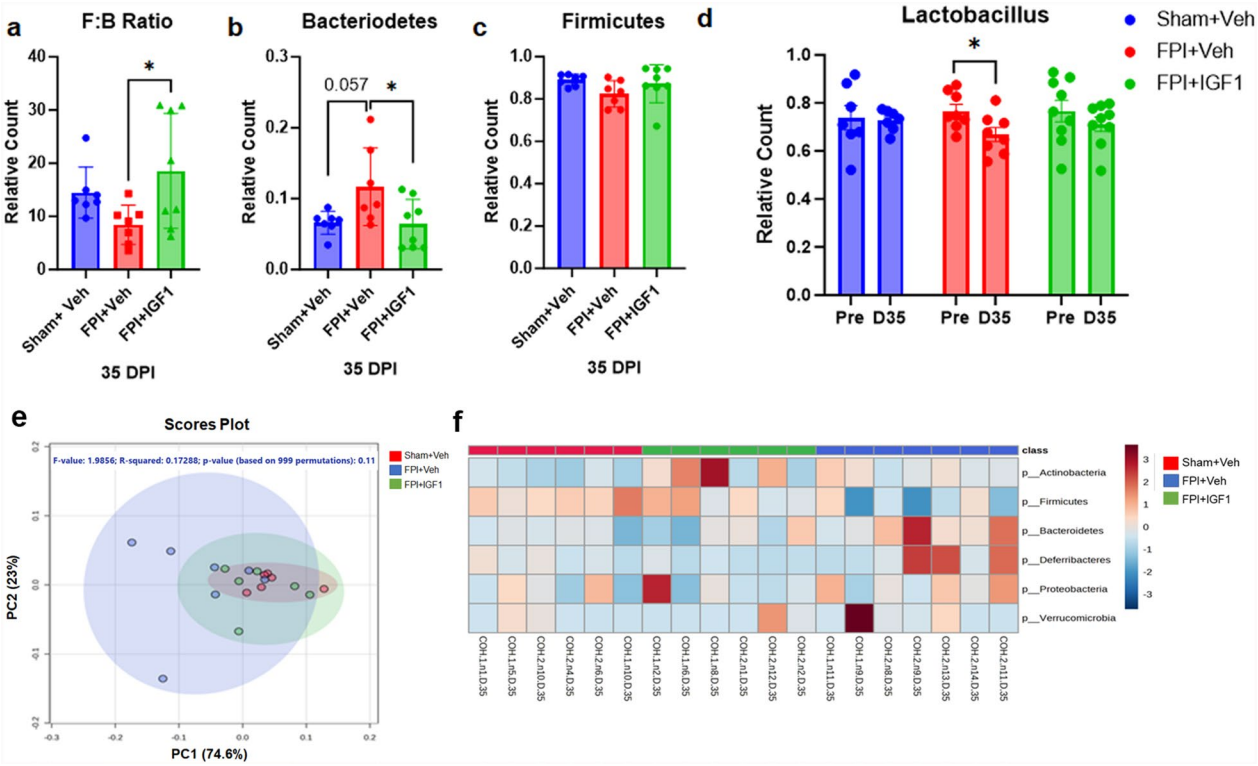

Fig. 5 Gut dysbiosis after FPI is improved by IGF-1. Gut bacterial composition was assessed from fecal samples at 35 DPI. The ratio of Firmicutes to Bacteroidetes (F:B), an estimate of gut health, was significantly increased in the FPI + IGF-1 treated rats compared to the FPI + Veh rats ($p < 0.05$) (**a**). The relative count of Bacteriodetes was increased in FPI + Veh rats ($p = 0.057$, NS vs. Sham + Veh), and this was significantly reduced with IGF-1 treatment ($p < 0.05$ vs. FPI + Veh) (**b**). There were no significant changes identified in Firmicutes (**c**). In **d**, the abundance of *Lactobacillus* was significantly decreased in the FPI + Veh rats at 35 DPI compared to baseline ($p < 0.05$), while there were no significant differences identified at 35 DPI in either the Sham + Veh or FPI + IGF-1 groups. In **e**, principal component analysis (PCA) using the partial Least-Squares Discriminant Analysis (PLS-DA shows that the major phyla for Sham + Veh and FPI + IGF-1 rats cluster more closely together than do the FPI + Veh. In **f**, heat map expression levels further demonstrate that FPI + Veh rats have an altered gut bacterial repertoire, compared to Sham + Veh, and that the FPI + IGF-1 rats are more similar to sham rats. Data are represented as Mean ± SEM; n = 4–5 per group. *$p < 0.05$; **$p < 0.01$

improving gut structure and function may underlie functional CNS improvements [107]. Increased gut permeability and elevated plasma LPS have been shown to be associated with cognitive decline [108, 109]. That IGF-1 treatment after FPI ameliorated the elevated plasma iFABP, LPS, and Muc-2, suggests that IGF-1 may be acting on the blood-gut-barrier, as has been previously described [71, 110–112]. The IGF-1 treatment may have also acted on the protective mucous barrier [113] because the FPI-induced decrease in goblet cells after injury was mitigated by IGF-1 treatment. It was surprising that IGF-1 reduced the number of Ki67 + progenitor cells in the intestinal crypts, despite its positive influence on permeability, the goblet cells, and dysmorphia. It is possible that FPI altered enterocyte survival or influenced the types of cellular offspring being produced by the progenitor cells, accounting for the goblet cell loss and dysmorphia. Future studies are needed to more fully examine the cellular make-up, turnover rates, and function of the intestines in response to injury and treatments. Considering the fact that TBI results in dysmotility and gastroparesis in the clinic [99, 100, 114] and animal models [115], the effects of IGF-1 on gut motility also need to be explored.

Numerous clinical and preclinical studies support the notion that gut dysmorphia can be targeted to improve neurological function. In multiple sclerosis, treating the gut improved neurobehavioral performance and prevented the loss of myelin [116–118]. In a mouse model of obesity, β-glucan administered into the lower GI tract attenuates colonic barrier dysfunction, inflammation, and cognitive and affective impairment [119]. In animal models of PD and AD, restoring gut structure and function mitigated the genetically induced neurodegeneration and neurobehavioral impairment [120–122]. Furthermore, targeting stroke-induced intestinal dysfunction using IESCs was beneficial to post-stroke outcomes [123]. Therefore, the gut appears

to be an important therapeutic target in TBI and other neurological disorders.

Increased neurogenesis after brain insults has been shown to result in aberrant growth and integration into hippocampal circuitry, resulting in impaired hippocampal function [74, 77, 85, 124]. In the current study, FPI resulted in an increased number of DCX-labeled immature neurons in the hippocampus at 3 DPI, and this increase was partially ameliorated by IGF-1 treatment. This is consistent with previous studies in different models of TBI that have demonstrated elevated adult hippocampal neurogenesis after TBI [125, 126]. While FPI did increase immature neurons at 3 DPI, no such change in Ki67 proliferating cells were observed in the dentate gyrus at 3 DPI. There are several possible explanations for this observation. Although the number of proliferating cells was not increased by FPI, it is possible that the rate of proliferation was increased, or that the generation of immature neurons as opposed to astrocytes is increased, as has been previously described [76, 126]. Consistent with this possibility, enhanced proliferation after TBI has been recorded within 1 and 14 DPI [76, 127–129]. It is possible that had earlier or later post-FPI timepoints been examined, the results may have been different. Another possibility is that FPI promotes survival of immature neurons, rather than increased proliferation, yielding a net increase in the number of DCX-labeled immature neurons, but not in Ki67 + cells. Consistent with this possibility, TBI has been previously shown to enhance both the survival and dendritic outgrowth of immature neurons in the adult hippocampus [74, 75, 85, 125]. Importantly, IGF-1has been previously shown to normalize TBI-induced alterations to adult hippocampal neurogenesis [46], consistent with the current study.

While the current findings have intriguing therapeutic implications for TBI, there are several limitations. In addition to obvious endocrine differences, there are documented sex differences in the response to TBI, in both clinical studies [130–135] and animal models [136–140]. This includes sex differences in the effects on the gut and the influence of gut microbiota on recovery after injury [141]. Because this study only looked at male rats, it is unclear what the differences would be in female rats. Furthermore, the use of IGF-1 in humans is limited clinically as it can cause hypoglycemia in non-diabetic individuals [48, 142], and such metabolic effects of IGF-1 treatment after FPI may have influenced the observed results. Nevertheless, this and other preclinical and clinical studies support the benefit of IGF-1 after FPI, and the current study establishes the possibility that IGF-1 signaling in the gut can be targeted to treat post-traumatic outcomes. Future studies can more selectively target IGF-1 signaling components to achieve therapeutic effects without toxic side effects.

In conclusion, the current findings highlight the benefit of systemic IGF-1 treatment after FPI in rats for improving gut permeability, dysmorphia, altered microbiome, and normalizing the FPI-induced increase in adult hippocampal neurogenesis. Considering the growing recognition of the importance of gut function on neurological outcomes, as well as the multitude of studies indicating gut dysfunction after TBI, these findings support further interrogation of IGF-1 signaling after TBI. The results also suggest the exciting possibility that gut dysmorphia and dysfunction may be novel therapeutic targets for improving TBI outcomes. Future studies are needed to more fully explore these possibilities.

Methods

Animals

10-week-old male Sprague–Dawley rats (Total = 36 rats) were used for this study. At one week prior to FPI or sham, rats were housed in individual cages under controlled environment with a 12-h light dark cycle (light on at 6:00 and light off at 18:00), with food and water continuously available and maintained on a standard diet (Envigo # 8604) for the duration of the experiment. Rats were randomly assigned into three groups: Sham + Veh, FPI + Veh, and FPI + IGF-1. Rats were administered with vehicle (Veh) or recombinant human (rh)IGF-1 (R&D Systems #291-G1-01 M) via i.p. injection (200 µg in 500 µL Phosphate Buffered Saline (PBS)) at 4 h and 24 h post-FPI. This dose was selected based on reports showing that it improved intestinal and neurobehavioral outcomes in a rat stroke model [110]. All Veh rats were given equal volume PBS in place of IGF-1. A subset of rats from each treatment group (n = 7–10 per group) were sacrificed at 3 DPI for assessment of gut pathology and permeability. Additional rats (n = 3–4 per group) were sacrificed at 35 DPI for assessment of gut morphology. All rat experimental protocols were approved by the Institutional Animal Care and Use Committee (IACUC) of Texas A&M Health Science Center (AUP #2010–0140) (Fig. 6).

Fluid percussion injury (FPI)

A mild-to-moderate lateral FPI was used as a model of TBI, as previously described [74, 86, 143]. Rats were initially anesthetized in an induction chamber (pre-filled with 4% isoflurane in 100% O_2) and later the level of the isoflurane was reduced to 2% for maintenance. Under anesthesia, the hair on the top of the rat's head

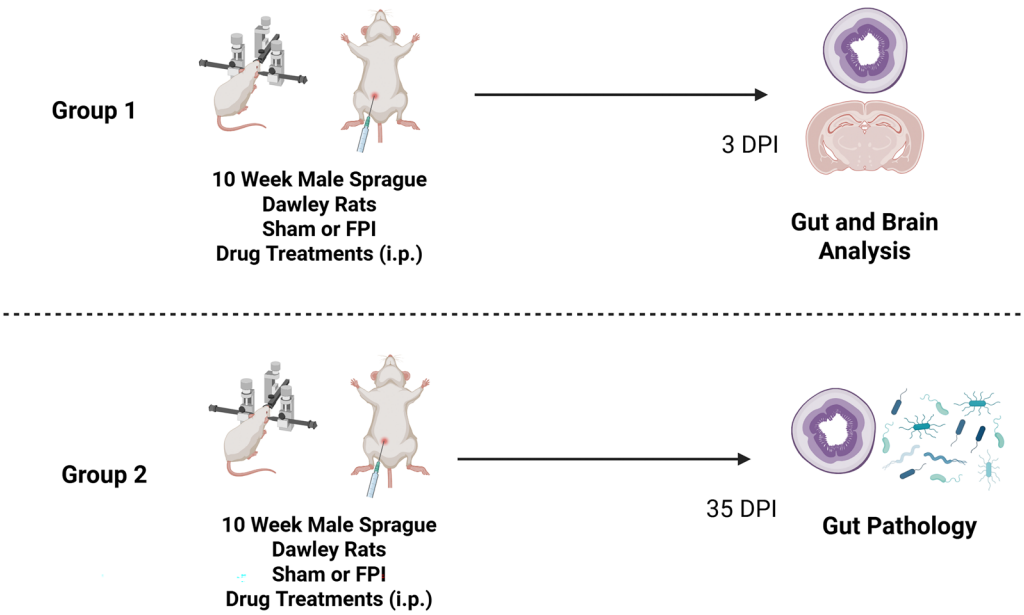

Fig. 6 Experimental Design for the study. Schematic diagram depicting the experimental design showing that rats received either sham or FPI at 10-weeks-of age, followed by IGF-1 or vehicle at 4 and 24 hours after surgery. Tissue was then collected for analysis at either 3 or 35 days post injury (DPI)

was trimmed as close to the skin as possible. Rats were placed in a stereotaxic instrument (Stoelting, Illinois) and a 2-mm burr hole was drilled on the skull using drill bits (Stoelting, Illinois) over the left parietal cortex, at -2 mm antero-posterior to bregma and 3 mm medio-lateral to midline [144], ensuring that dura remained intact. A female Luer-Lok cannula was secured to the skull with dental cement (PlasticOne), then rats were connected to the fluid percussion instrument (Custom Design and Fabrication, Richmond, VA; Model 01-B) via male Luer-Lok attachment. The rat was placed on its side and breathing was monitored. Once a normal breathing pattern resumed, but prior to the rat regaining complete consciousness, the pendulum of the FPI device was released to cause a single ~ 2 atm pressure pulse injury, as measured by a digital Oscilloscope (Tenma model # 728395), connected to a signal transducer hooked in-line between the fluid percussion cylinder and the syringe. Sham animals all underwent the same procedures, but the pendulum was not released so no fluid pulse was delivered to the intact dura. Rats were monitored closely after injury, no death or loss of consciousness were observed, consistent with a mild-to-moderate injury.

Gut permeability ELISA assays

Serum was collected via saphenous draw at 3 days post-FPI from 26 rats (7 Sham + Veh, 9 FPI + Veh, 10 FPI + IGF1). ELISA assays were used to determine levels of surrogate measures of gut permeability: lipopolysaccharide (LPS) (Mybiosources, MBS268498; Detection range: 15.6 ng/mL–1000 ng/mL), mucin-2 (Muc-2) (Mybiosources, MBS2019254; Detection range: 0.312–20 ng/mL), and intestinal fatty acid binding protein (iFABP) (Mybiosources, MBS3807789; Detection range: 1–3200 pg/mL). The procedure was performed according to the manufacturer's directions. Plates were read on a microplate reader (450 nm; TECAN, VT) and the concentration of the samples was obtained by interpolation from the standard curve.

Gut histology

At 3 or 35 DPI, a portion of the distal ileum and proximal colon were dissected, fixed in 4% PFA, and embedded in paraffin. Paraffin sections (10 µm) were collected on glass slides and analyzed for immunohistochemistry, hematoxylin and eosin (H&E), and Periodic acid-Schiff (PAS) staining [145]. For H&E and PAS staining, sections were photographed at 20 × magnification with the VS200 slide scanner (Olympus) and scored by a rater blind to the subject's condition. The length was measured from the tip of the villi to the base at the crypt, and the width was measured at the midpoint of the height [146]. The number of crypts at the base of each villus was also counted, as previously described [110]. A total of three slides, with 3 ileum or colon slices per slide were used for each rat. Four positions were selected for each image and 3 villi were measured from each position. All analysis was

done on the OlyVia software using the line measurement tool. The data presented are an average of these measurements. At 3 DPI, measurements were done for 14 rats (4 Sham + Veh, 5 FPI + Veh, 5 FPI + IGF1). At 35 DPI, assessments were taken from 10 rats (3 Sham + Veh, 3 FPI + Veh, 4 FPI + IGF1).

Gut immunohistochemistry

Immunofluorescence for KI67 was performed as previously described [123]. Briefly, a portion of the ileum was embedded in paraffin (Leica Microsystems, Buffalo Grove, IL, USA) and stored at room temperature until use. Paraffin sections (10 µm) were collected on glass slides and incubated in blocking buffer (5%BSA + 0.1% Triton X-100 in PBS, pH 7.4) for 20 min at room temperature. Sections were incubated overnight at 4 °C with primary rabbit anti-Ki67 (1:250, Abcam, ab16667). Secondary antibody (Alexa Fluor 555 goat anti-rabbit, Invitrogen) was used at 1:1000 dilution for 1 h at room temperature. Sections were washed three times in PBS, and cover slipped with mounting media containing the nuclear dye DAPI (Fluoroshield, Abcam, ab228549). Sections were imaged using a fluorescent microscope (Olympus, Bethlehem, PA). Gut sections probed for Ki67 immunohistochemistry were imaged and coded and then scored by a rater blinded to the experimental condition. Slides were scored using a predefined scale from 1 to 5 according to staining localization and brightness along the crypt cells. A minimum of 3 sections were scored for each rat, and the data presented are an average of these 3 sections. At 3 DPI, measurements were done for 14 rats (4 Sham + Veh, 5 FPI + Veh, 5 FPI + IGF1). At 35 DPI, assessments were taken from 10 rats (3 Sham + Veh, 3 FPI + Veh, 4 FPI + IGF1).

Microbiome analysis

Microbiome analysis was conducted using fecal samples collected at baseline (pre-FPI) and 35 days after FPI from 12 rats (3 Sham + Veh, 3 FPI + Veh, 6 FPI + IGF1). The fecal samples were frozen immediately after collection and stored at − 80 °C until shipping to Diversigen (New Brighton, MN). Briefly, DNA was extracted with Qiagen's DNeasy PowerSoil Pro Kit (Qiagen, Germantown, MD) automated for high throughput on QiaCube HT (Qiagen, Germantown, MD), with bead beating in Qiagen Powerbead Pro plates (Qiagen, Germantown, MD) and quantified with Qiant-iT Picogreen dsDNA Assay (Invitrogen, Carlsbad, CA). Libraries were prepared with a procedure adapted from the Nextera Library Prep kit (Illumina, San Diego, CA) and sequenced on an Illumina NovaSeq using single-end 1 × 100 reads (Illumina, San Diego, CA). DNA sequences were filtered for low quality (Q-Score < 30) and length (< 50), and adapter sequences were trimmed using cutadapt. Fastq files were converted into a single fasta using shi7. Sequences were trimmed to a maximum length of 100 bp prior to alignment. DNA sequences were aligned to a curated database containing all representative genomes in RefSeq for bacteria with additional manually curated strains. Alignments were made at 97% identity against all reference genomes (Diversigen's Venti database) using fully gapped alignment with BURST. Ties were broken by minimizing the overall number of unique Operational Taxonomic Units (OTUs). For taxonomy assignment, each input sequence was assigned to the lowest common ancestor that was consistent across at least 80% of all reference sequences tied for best hit. The number of counts for each out was normalized to the average genome length. OTUs accounting for less than one millionth of all species-level markers and those with less than 0.01% of their unique genome regions covered (and < 1% of the whole genome) were discarded. Absolute count data was then used to calculate Firmicutes: Bacteroidetes ratio, and abundance of specific bacterial groups was evaluated.

Immunohistochemistry for hippocampal proliferation and neurogenesis

Because IGF-1 is known to influence numerous cell types, it is possible that the i.p. injections could have passed through the blood–brain barrier and influenced dividing cells in the central nervous system. Therefore, this study also examined the hippocampus, a region of the adult rat brain in which ongoing neurogenesis is observed. Proliferating cells in the dentate gyrus were examined as 3 DPI, as were the number of immature neurons in the dentate gyrus using doublecortin (DCX), a marker of immature neurons. Immunohistochemistry for DCX and Ki67 were performed as previously described [74, 143, 147, 148]. Briefly, rats were anesthetized with Fatal Plus (Sodium Pentobarbital; 52 mg/kg, administered i.p.) and transcardially perfused with phosphate buffered saline (PBS) through the left ventricle until the blood ran clear. This was followed by 4% paraformaldehyde (PFA) through the left ventricle. All brains were allowed to postfix in the skull for 24 h in PFA, after which they were extracted and fixed for an additional 24 h in 4% PFA. Fixed brains were cut into 44-µm thick serial sections with a freezing microtome (American Optical Corp; Model #860). Slices were first incubated in a 1X Citrate Buffer (Millipore Sigma) for 1 h at 45 °C. Slices were then washed and stained with goat anti-DCX antibody (Santa Cruz Inc. USA) or rabbit anti-Ki67 (1:250, Abcam, ab16667) overnight at room temperature, rotating. After overnight incubation, slices were washed and stained with a secondary biotinylated goat anti-Rabbit IgG (Alexaflour-555; 1:200) (Ki67) or secondary donkey

anti-Goat IgG (AlexFlour-555; 1:200) (DCX). Slices were mounted and cover-slipped with antifade reagent containing DAPI (Vector Laboratories #H-1200-10).

Imaging for all immunohistochemistry was done on a fluorescent microscope (Olympus, Bethlehem, PA). Unbiased stereology-based analysis was used to quantify cells positive for DCX in the hippocampus, as previously described [74, 147, 148]. Sections (~every 260–350 µm apart) containing the dorsal hippocampus (Bregma −1.34 through −2.80) were selected for analysis. Analysis of DCX+cells was performed in the ipsilateral infra- and supra-pyramidal blades of the dentate gyrus granule cell layer/subgranular zone. Total Ki67+cells in the entire dentate gyrus were manually counted, and all counts were conducted by raters blind to experimental conditions. A minimum of 3 left (ipsilateral to injury) hippocampi were counted per animal, per antibody, within the stereological coordinates indicated above. Analysis was completed for 14 rats (4 Sham+Veh, 5 FPI+Veh, 5 FPI+IGF1).

Statistical analysis

Prior to statistical analysis, data were analyzed for outliers using the ROUT algorithm in GraphPad Prism, Q=1% [147, 149], and outliers were removed from all associated measurements. Data for all groups were analyzed by one-way analysis of variance (ANOVA) with comparisons between groups performed using post-hoc Tukey test. All statistical analysis was performed using GraphPad Prism (Version 9.0; GraphPad). Significance for all tests was set at $p<0.05$ and a trend was considered at $0.10\geq p>0.05$.

Abbreviations

CCI	Controlled cortical impact
DPI	Days post-injury
FPI	Fluid percussion injury
GH	Growth hormone
GI	Gastrointestinal
HPA	Hypothalamic pituitary axis
iFABP	Intestinal fatty acid binding protein
IGF-1	Insulin-like growth factor
IGFBP	Insulin-like growth factor binding protein
i.p.	Intraperitoneal
LPS	Lipopolysaccharide
Muc-2	Mucin-2
TBI	Traumatic brain injury
Veh	Vehicle

Supplementary Information

The online version contains supplementary material available at https://doi.org/10.1186/s40478-025-01998-x.

Supplementary file 1.

Acknowledgements

The authors acknowledge Reuben Gelin and Carla Furbeck for their assistance in scoring gut pathology, and Samantha Beevers and Brooke Heckel for their assistance collecting tissue samples. The authors would also like to acknowledge Dr. Malea Murphy and the Integrated Microscopy & Imaging Laboratory (IMIL) at the Texas A&M College of Medicine. The schematic diagram was created using biorender.com.

Author contributions

LV: investigation, Writing—Original Draft, project administration. JI: methodology, formal analysis, Writing—Original Draft, Writing—Editing & Review. AP: formal analysis, investigation, data curation, Writing—Original Draft, visualization. JH: investigation, visualization. EH: investigation. AI: investigation. RD: investigation. YE: methodology. KKM: methodology. AD: formal analysis. RP: methodology, formal analysis. FS: conceptualization, resources, Writing—Editing & Review, funding acquisition. LAS: conceptualization, resources, Writing—Original Draft, Writing—Editing & Review, supervision, funding acquisition. All authors read and approved the final manuscript.

Funding

This work was supported by funding from Texas A&M Neural-Gut Immune Axis group and the WoodNext Foundation.

Availability of data and materials

The datasets used and/or analyzed during the current study are available from the corresponding author on reasonable request.

Declarations

Ethics approval and consent to participate

All the animal experimental protocols were approved by the Institutional Animal Care Committee (IACUC) of Texas A&M Health Science Center (AUP #2010-0140).

Consent for publication

Not applicable.

Competing interests

The authors declare no competing interests.

Author details

[1]Department of Neuroscience and Experimental Therapeutics, College of Medicine, Texas A and M University, 8447 Riverside Pkwy, Bryan, TX 77807-3260, USA. [2]Department of Statistics, College of Arts and Sciences, Texas A and M University, College Station, TX, USA. [3]Gastrointestinal Laboratory, College of Veterinary Medicine and Biomedical Sciences, Texas A and M University, College Station, TX, USA.

Received: 3 February 2025 Accepted: 3 April 2025
Published online: 03 May 2025

References

1. Maas AIR et al (2017) Traumatic brain injury: integrated approaches to improve prevention, clinical care, and research. Lancet Neurol 16(12):987–1048
2. Coronado VG et al (2012) Trends in traumatic brain injury in the U.S. and the public health response: 1995–2009. J Saf Res 43(4):299–307
3. Ahmed S et al (2017) Traumatic brain injury and neuropsychiatric complications. Indian J Psychol Med 39(2):114–121
4. Collaborators GUND (2021) Burden of neurological disorders across the US from 1990–2017: a global burden of disease study. JAMA Neurol 78(2):165–176
5. Elser H et al (2023) Head injury and long-term mortality risk in community-dwelling adults. JAMA Neurol 80(3):260–269
6. Nordström A, Nordström P (2018) Traumatic brain injury and the risk of dementia diagnosis: a nationwide cohort study. PLoS Med 15(1):e1002496
7. Agha A et al (2004) Anterior pituitary dysfunction in survivors of traumatic brain injury. J Clin Endocrinol Metab 89(10):4929–4936

8. Olivecrona Z, Dahlqvist P, Koskinen LO (2013) Acute neuro-endocrine profile and prediction of outcome after severe brain injury. Scand J Trauma Resusc Emerg Med 21:33
9. Popovic V et al (2004) Hypopituitarism as a consequence of traumatic brain injury (TBI) and its possible relation with cognitive disabilities and mental distress. J Endocrinol Invest 27(11):1048–1054
10. Yang WH et al (2016) Endocrine dysfunction following traumatic brain injury: a 5-year follow-up nationwide-based study. Sci Rep 6:32987
11. Kelly DF et al (2000) Hypopituitarism following traumatic brain injury and aneurysmal subarachnoid hemorrhage: a preliminary report. J Neurosurg 93(5):743–752
12. Briet C et al (2019) Should we assess pituitary function in children after a mild traumatic brain injury? A Prospect Study Front Endocrinol (Lausanne) 10:149
13. Kaulfers AM et al (2010) Endocrine dysfunction following traumatic brain injury in children. J Pediatr 157(6):894–899
14. Bromberg CE et al (2020) Sex-dependent pathology in the HPA axis at a sub-acute period after experimental traumatic brain injury. Front Neurol 11:946
15. Taheri S et al (2022) The role of apoptosis and autophagy in the hypothalamic-pituitary-adrenal (HPA) axis after traumatic brain injury (TBI). Int J Mol Sci 23(24):15699
16. Javed Z, Qamar U, Sathyapalan T (2015) Pituitary and/or hypothalamic dysfunction following moderate to severe traumatic brain injury: current perspectives. Indian J Endocrinol Metab 19(6):753–763
17. Larkin S, Ansorge O (2017) Development and microscopic anatomy of the pituitary gland
18. Chen X et al (2011) Methylprednisolone exacerbates acute critical illness-related corticosteroid insufficiency associated with traumatic brain injury in rats. Brain Res 1382:298–307
19. Tanriverdi F et al (2010) Investigation of antihypothalamus and antipituitary antibodies in amateur boxers: is chronic repetitive head trauma-induced pituitary dysfunction associated with autoimmunity? Eur J Endocrinol 162(5):861–867
20. Cohan P et al (2005) Acute secondary adrenal insufficiency after traumatic brain injury: a prospective study*. Crit Care Med 33(10):2358–2366
21. Kreber LA, Griesbach GS, Ashley MJ (2016) Detection of growth hormone deficiency in adults with chronic traumatic brain injury. J Neurotrauma 33(17):1607–1613
22. Tanriverdi F et al (2006) High risk of hypopituitarism after traumatic brain injury: a prospective investigation of anterior pituitary function in the acute phase and 12 months after trauma. J Clin Endocrinol Metab 91(6):2105–2111
23. Bondanelli M et al (2004) Occurrence of pituitary dysfunction following traumatic brain injury. J Neurotrauma 21(6):685–696
24. Madathil SK, Evans HN, Saatman KE (2010) Temporal and regional changes in IGF-1/IGF-1R signaling in the mouse brain after traumatic brain injury. J Neurotrauma 27(1):95–107
25. Mangiola A et al (2015) Role and importance of IGF-1 in traumatic brain injuries. Biomed Res Int 2015:736104
26. Hatton J et al (1997) Intravenous insulin-like growth factor-I (IGF-I) in moderate-to-severe head injury: a phase II safety and efficacy trial. J Neurosurg 86(5):779–786
27. Hatton J et al (2006) Systemic metabolic effects of combined insulin-like growth factor-I and growth hormone therapy in patients who have sustained acute traumatic brain injury. J Neurosurg 105(6):843–852
28. Rockich KT et al (1999) Effect of recombinant human growth hormone and insulin-like growth factor-1 administration on IGF-1 and IGF-binding protein-3 levels in brain injury. Pharmacotherapy 19(12):1432–1436
29. Yakar S et al (2002) Circulating levels of IGF-1 directly regulate bone growth and density. J Clin Investig 110(6):771–781
30. Logan A, Oliver JJ, Berry M (1994) Growth factors in CNS repair and regeneration. Prog Growth Factor Res 5(4):379–405
31. Kazanis I et al (2004) Alterations in IGF-I, BDNF and NT-3 levels following experimental brain trauma and the effect of IGF-I administration. Exp Neurol 186(2):221–234
32. Beilharz EJ et al (1995) Insulin-like growth factor II is induced during wound repair following hypoxic-ischemic injury in the developing rat brain. Brain Res Mol Brain Res 29(1):81–91
33. Mueller RV et al (1994) The effect of insulinlike growth factor I on wound healing variables and macrophages in rats. Arch Surg 129(3):262–265
34. Schwab S et al (1997) Plasma insulin-like growth factor I and IGF binding protein 3 levels in patients with acute cerebral ischemic injury. Stroke 28(9):1744–1748
35. Jeevanandam M, Holaday NJ, Petersen SR (1995) Plasma levels of insulin-like growth factor binding protein-3 in acute trauma patients. Metabolism 44(9):1205–1208
36. Wagner J et al (2010) Acute gonadotroph and somatotroph hormonal suppression after traumatic brain injury. J Neurotrauma 27(6):1007–1019
37. Zgaljardic DJ et al (2011) Serum IGF-1 concentrations in a sample of patients with traumatic brain injury as a diagnostic marker of growth hormone secretory response to glucagon stimulation testing. Clin Endocrinol (Oxf) 74(3):365–369
38. Robles JF et al (2009) Traumatic injury to the brain and endocrine evaluation of the anterior pituitary a year after the event (The TRIBE Study). Int J Endocrinol Metab 7(2):72–81
39. Sanus GZ et al (2007) Cerebrospinal fluid and serum levels of insulin-like growth factor-1 and insulin-like growth factor binding protein-3 in patients with severe head injury. Ulus Travma Acil Cerrahi Derg 13(4):281–287
40. Feeney C et al (2017) Serum insulin-like growth factor-I levels are associated with improved white matter recovery after traumatic brain injury. Ann Neurol 82(1):30–43
41. Rao A et al (2023) Endocrine abnormalities in children with traumatic brain injury at a tertiary care center. Cureus 15(1):e34131
42. Greco T, Hovda D, Prins M (2013) The effects of repeat traumatic brain injury on the pituitary in adolescent rats. J Neurotrauma 30(23):1983–1990
43. Ozdemir D et al (2012) Relationship between circulating IGF-1 levels and traumatic brain injury-induced hippocampal damage and cognitive dysfunction in immature rats. Neurosci Lett 507(1):84–89
44. Corne R et al (2021) Insulin-like growth factors may be markers of both traumatic brain injury and fear-related stress. Neuroscience 466:205–221
45. Saatman KE et al (1997) Insulin-like growth factor-1 (IGF-1) improves both neurological motor and cognitive outcome following experimental brain injury. Exp Neurol 147(2):418–427
46. Carlson SW, Saatman KE (2018) Central infusion of insulin-like growth factor-1 increases hippocampal neurogenesis and improves neurobehavioral function after traumatic brain injury. J Neurotrauma 35(13):1467–1480
47. Rubovitch V et al (2010) The intricate involvement of the insulin-like growth factor receptor signaling in mild traumatic brain injury in mice. Neurobiol Dis 38(2):299–303
48. Sherwin RS, Borg WP, Boulware SD (1994) Metabolic effects of insulin-like growth factor I in normal humans. Horm Res 41(Suppl 2):97–101
49. Bansal V et al (2009) Traumatic brain injury and intestinal dysfunction: uncovering the neuro-enteric axis. J Neurotrauma 26(8):1353–1359
50. DeSana AJ et al (2024) Acute gastrointestinal permeability after traumatic brain injury in mice precedes a bloom in Akkermansia muciniphila supported by intestinal hypoxia. Sci Rep 14(1):2990
51. Katzenberger RJ, Ganetzky B, Wassarman DA (2015) The gut reaction to traumatic brain injury. Fly (Austin) 9(2):68–74
52. Zhu CS et al (2018) A review of traumatic brain injury and the gut microbiome: insights into novel mechanisms of secondary brain injury and promising targets for neuroprotection. Brain Sci 8(6):113
53. Frankot MA et al (2023) Acute gut microbiome changes after traumatic brain injury are associated with chronic deficits in decision-making and impulsivity in male rats. Behav Neurosci 137(1):15–28
54. Urban RJ et al (2020) Altered fecal microbiome years after traumatic brain injury. J Neurotrauma 37(8):1037–1051
55. Mahajan C et al (2023) Characteristics of gut microbiome after traumatic brain injury. J Neurosurg Anesthesiol 35(1):86–90

56. Taraskina A et al (2022) Effects of traumatic brain injury on the gut microbiota composition and serum amino acid profile in rats. Cells 11(9):1409
57. Brenner LA et al (2020) Microbial diversity and community structures among those with moderate to severe TBI: a united states-veteran microbiome project study. J Head Trauma Rehabil 35(5):332–341
58. Nicholson SE et al (2019) Moderate traumatic brain injury alters the gastrointestinal microbiome in a time-dependent manner. Shock 52(2):240–248
59. Treangen TJ et al (2018) Traumatic brain injury in mice induces acute bacterial dysbiosis within the fecal microbiome. Front Immunol 9:2757
60. Wang S et al (2021) The association of traumatic brain injury, gut microbiota and the corresponding metabolites in mice. Brain Res 1762:147450
61. Soriano S et al (2022) Alterations to the gut microbiome after sport-related concussion in a collegiate football players cohort: a pilot study. Brain Behav Immun Health 21:100438
62. Zheng Y et al (2018) Intestinal epithelial cell-specific IGF1 promotes the expansion of intestinal stem cells during epithelial regeneration and functions on the intestinal immune homeostasis. Am J Physiol Endocrinol Metab 315(4):E638-e649
63. Rowland KJ, Choi PM, Warner BW (2013) The role of growth factors in intestinal regeneration and repair in necrotizing enterocolitis. Semin Pediatr Surg 22(2):101–111
64. D'Addio F et al (2015) Circulating IGF-I and IGFBP3 levels control human colonic stem cell function and are disrupted in diabetic enteropathy. Cell Stem Cell 17(4):486–498
65. Bohin N et al (2020) Insulin-like growth factor-1 and mTORC1 signaling promote the intestinal regenerative response after irradiation injury. Cell Mol Gastroenterol Hepatol 10(4):797–810
66. Howarth GS, Xian CJ, Read LC (1998) Insulin-like growth factor-I partially attenuates colonic damage in rats with experimental colitis induced by oral dextran sulphate sodium. Scand J Gastroenterol 33(2):180–190
67. Qiu W et al (2010) Growth factors protect intestinal stem cells from radiation-induced apoptosis by suppressing PUMA through the PI3K/AKT/p53 axis. Oncogene 29(11):1622–1632
68. Van Landeghem L et al (2015) IGF1 stimulates crypt expansion via differential activation of 2 intestinal stem cell populations. Faseb j 29(7):2828–2842
69. Wilkins HR et al (2002) Reduction of spontaneous and irradiation-induced apoptosis in small intestine of IGF-I transgenic mice. Am J Physiol Gastrointest Liver Physiol 283(2):G457–G464
70. Zhou W, Rowitz BM, Dailey MJ (2018) Insulin/IGF-1 enhances intestinal epithelial crypt proliferation through PI3K/Akt, and not ERK signaling in obese humans. Exp Biol Med 243(11):911–916
71. Lorenzo-Zúñiga V et al (2006) Insulin-like growth factor I improves intestinal barrier function in cirrhotic rats. Gut 55(9):1306–1312
72. van Goudoever JB et al (2008) The impact of enteral insulin-like growth factor 1 and nutrition on gut permeability and amino acid utilization. J Nutr 138(9):1829s–1833s
73. Ma Y et al (2019) Lactobacillus acidophilus exerts neuroprotective effects in mice with traumatic brain injury. J Nutr 149(9):1543–1552
74. Shapiro LA (2017) Altered hippocampal neurogenesis during the first 7 days after a fluid percussion traumatic brain injury. Cell Transplant 26(7):1314–1318
75. Clark LR et al (2020) Mild traumatic brain injury induces transient, sequential increases in proliferation, neuroblasts/immature neurons, and cell survival: a time course study in the male mouse dentate gyrus. Front Neurosci 14:612749
76. Dash PK, Mach SA, Moore AN (2001) Enhanced neurogenesis in the rodent hippocampus following traumatic brain injury. J Neurosci Res 63(4):313–319
77. Neuberger EJ et al (2017) Enhanced dentate neurogenesis after brain injury undermines long-term neurogenic potential and promotes seizure susceptibility. Stem Cell Rep 9(3):972–984
78. Trøseid M et al (2013) Plasma lipopolysaccharide is closely associated with glycemic control and abdominal obesity: evidence from bariatric surgery. Diabetes Care 36(11):3627–3632
79. Volynets V et al (2016) Assessment of the intestinal barrier with five different permeability tests in healthy C57BL/6J and BALB/cJ mice. Dig Dis Sci 61(3):737–746
80. Sikora M et al (2019) Intestinal fatty acid binding protein, a biomarker of intestinal barrier, is associated with severity of psoriasis. J Clin Med 8(7):1021
81. Mazarati A et al (2021) Disruption of intestinal barrier and endotoxemia after traumatic brain injury: Implications for post-traumatic epilepsy. Epilepsia 62(6):1472–1481
82. Lau E et al (2016) The role of I-FABP as a biomarker of intestinal barrier dysfunction driven by gut microbiota changes in obesity. Nutr Metab (Lond) 13:31
83. Johansson ME, Larsson JM, Hansson GC (2011) The two mucus layers of colon are organized by the MUC2 mucin, whereas the outer layer is a legislator of host-microbial interactions. Proc Natl Acad Sci U S A 108(Suppl 1):4659–4665
84. Pelaseyed T et al (2014) The mucus and mucins of the goblet cells and enterocytes provide the first defense line of the gastrointestinal tract and interact with the immune system. Immunol Rev 260(1):8–20
85. Chirumamilla S et al (2002) Traumatic brain injury induced cell proliferation in the adult mammalian central nervous system. J Neurotrauma 19(6):693–703
86. Robinson C, Apgar C, Shapiro LA (2016) Astrocyte hypertrophy contributes to aberrant neurogenesis after traumatic brain injury. Neural Plast 2016:1347987
87. Witgen BM et al (2005) Regional hippocampal alteration associated with cognitive deficit following experimental brain injury: a systems, network and cellular evaluation. Neuroscience 133(1):1–15
88. Coradduzza D et al (2023) Age-related cognitive decline, focus on microbiome: a systematic review and meta-analysis. Int J Mol Sci 24(18):13680
89. Grabrucker S et al (2023) Microbiota from Alzheimer's patients induce deficits in cognition and hippocampal neurogenesis. Brain 146(12):4916–4934
90. Stojanov S, Berlec A, Štrukelj B (2020) The influence of probiotics on the firmicutes/bacteroidetes ratio in the treatment of obesity and inflammatory bowel disease. Microorganisms 8(11):1715
91. Chung YE et al (2019) Exploration of microbiota targets for major depressive disorder and mood related traits. J Psychiatr Res 111:74–82
92. Zheng P et al (2016) Gut microbiome remodeling induces depressive-like behaviors through a pathway mediated by the host's metabolism. Mol Psychiatry 21(6):786–796
93. Jiang H et al (2015) Altered fecal microbiota composition in patients with major depressive disorder. Brain Behav Immun 48:186–194
94. Huang Y et al (2018) Possible association of Firmicutes in the gut microbiota of patients with major depressive disorder. Neuropsychiatr Dis Treat 14:3329–3337
95. Zhong Q et al (2022) Differential gut microbiota compositions related with the severity of major depressive disorder. Front Cell Infect Microbiol 12:907239
96. Saji N et al (2019) The relationship between the gut microbiome and mild cognitive impairment in patients without dementia: a cross-sectional study conducted in Japan. Sci Rep 9(1):19227
97. Sundman MH et al (2017) The bidirectional gut-brain-microbiota axis as a potential nexus between traumatic brain injury, inflammation, and disease. Brain Behav Immun 66:31–44
98. Harrison-Felix C et al (2006) Causes of death following 1 year postinjury among individuals with traumatic brain injury. J Head Trauma Rehabil 21(1):22–33
99. Kao CH et al (1998) Gastric emptying in head-injured patients. Am J Gastroenterol 93(7):1108–1112
100. Norton JA et al (1988) Intolerance to enteral feeding in the brain-injured patient. J Neurosurg 68(1):62–66
101. Houlden A et al (2016) Brain injury induces specific changes in the caecal microbiota of mice via altered autonomic activity and mucoprotein production. Brain Behav Immun 57:10–20
102. Celorrio M, Friess SH (2022) Gut-brain axis in traumatic brain injury: impact on neuroinflammation. Neural Regen Res 17(5):1007–1008

103. Opeyemi OM et al (2021) Sustained dysbiosis and decreased fecal short-chain fatty acids after traumatic brain injury and impact on neurologic outcome. J Neurotrauma 38(18):2610–2621
104. Ma EL et al (2017) Bidirectional brain-gut interactions and chronic pathological changes after traumatic brain injury in mice. Brain Behav Immun 66:56–69
105. Hang CH et al (2003) Alterations of intestinal mucosa structure and barrier function following traumatic brain injury in rats. World J Gastroenterol 9(12):2776–2781
106. Doney E et al (2022) Inflammation-driven brain and gut barrier dysfunction in stress and mood disorders. Eur J Neurosci 55(9–10):2851–2894
107. Meng D et al (2022) Rifaximin protects against circadian rhythm disruption-induced cognitive impairment through preventing gut barrier damage and neuroinflammation. J Neurochem 163(5):406–418
108. Rundek T et al (2021) Gut permeability and cognitive decline: a pilot investigation in the northern manhattan study. Brain Behav Immun Health 12:100214
109. Pei Y et al (2023) Gut microbiota and intestinal barrier function in subjects with cognitive impairments: a cross-sectional study. Front Aging Neurosci 15:1174599
110. El-Hakim Y et al (2024) Peripheral, but not central, IGF-1 treatment attenuates stroke-induced cognitive impairment in middle-aged female sprague dawley rats: the gut as a therapeutic target. Brain Behav Immun 122:150–166
111. He Y et al (2018) Activation of IGF-1/IGFBP-3 signaling by berberine improves intestinal mucosal barrier of rats with acute endotoxemia. Fitoterapia 124:200–205
112. Chen T et al (2015) Insulin-like growth factor-1 contributes to mucosal repair by β-arrestin2-mediated extracellular signal-related kinase signaling in experimental colitis. Am J Pathol 185(9):2441–2453
113. Gustafsson JK, Johansson MEV (2022) The role of goblet cells and mucus in intestinal homeostasis. Nat Rev Gastroenterol Hepatol 19(12):785–803
114. Tan M, Zhu JC, Yin HH (2011) Enteral nutrition in patients with severe traumatic brain injury: reasons for intolerance and medical management. Br J Neurosurg 25(1):2–8
115. Olsen AB et al (2013) Effects of traumatic brain injury on intestinal contractility. Neurogastroenterol Motility 25:593
116. Camara-Lemarroy CR et al (2018) The intestinal barrier in multiple sclerosis: implications for pathophysiology and therapeutics. Brain 141(7):1900–1916
117. Lee YK et al (2011) Proinflammatory T-cell responses to gut microbiota promote experimental autoimmune encephalomyelitis. Proc Natl Acad Sci U S A 108(Suppl 1):4615–22
118. Secher T et al (2017) Oral administration of the probiotic strain escherichia coli nissle 1917 reduces susceptibility to neuroinflammation and repairs experimental autoimmune encephalomyelitis-induced intestinal barrier dysfunction. Front Immunol 8:1096
119. Shi H et al (2020) β-glucan attenuates cognitive impairment via the gut-brain axis in diet-induced obese mice. Microbiome 8(1):143
120. Sampson TR et al (2016) Gut microbiota regulate motor deficits and neuroinflammation in a model of parkinson's disease. Cell 167(6):1469-1480.e12
121. Lu Y et al (2023) Acanthopanax senticosus harms improves parkinson's disease by regulating gut microbial structure and metabolic disorders. Heliyon 9(7):e18045
122. Zhang Y et al (2023) Effect of gastrodin against cognitive impairment and neurodegeneration in APP/PS1 mice via regulating gut microbiota-gut-brain axis. Exp Brain Res 241(6):1661–1673
123. Mani KK et al (2023) Intestinal epithelial stem cell transplants as a novel therapy for cerebrovascular stroke. Brain Behav Immun 107:345–360
124. Correll EA et al (2021) Deficits in pattern separation and dentate gyrus proliferation after rodent lateral fluid percussion injury. IBRO Neurosci Rep 10:31–41
125. Villasana LE et al (2015) Functional integration of adult-born hippocampal neurons after traumatic brain injury(1,2,3). eNeuro. https://doi.org/10.1523/ENEURO.0056-15.2015
126. Bielefeld P et al (2024) Traumatic brain injury promotes neurogenesis at the cost of astrogliogenesis in the adult hippocampus of male mice. Nat Commun 15(1):5222
127. Urrea C et al (2007) Widespread cellular proliferation and focal neurogenesis after traumatic brain injury in the rat. Restor Neurol Neurosci 25(1):65–76
128. Sun D et al (2005) Cell proliferation and neuronal differentiation in the dentate gyrus in juvenile and adult rats following traumatic brain injury. J Neurotrauma 22(1):95–105
129. Rice AC et al (2003) Proliferation and neuronal differentiation of mitotically active cells following traumatic brain injury. Exp Neurol 183(2):406–417
130. Ma C et al (2019) Sex differences in traumatic brain injury: a multi-dimensional exploration in genes, hormones, cells, individuals, and society. Chinese Neurosurg J 5(1):24
131. Niemeier JP et al (2007) Gender differences in executive functions following traumatic brain injury. Neuropsychol Rehabil 17(3):293–313
132. Groswasser Z, Cohen M, Keren O (1998) Female TBI patients recover better than males. Brain Inj 12(9):805–808
133. Kirkness CJ et al (2004) Is there a sex difference in the course following traumatic brain injury? Biol Res Nurs 5(4):299–310
134. Farace E, Alves WM (2000) Do women fare worse: a metaanalysis of gender differences in traumatic brain injury outcome. J Neurosurg 93(4):539–545
135. Munivenkatappa A et al (2016) Traumatic brain injury: Does gender influence outcomes? Int J Crit Illn Inj Sci 6(2):70–73
136. Gupte R et al (2019) Sex Differences in traumatic brain injury: what we know and what we should know. J Neurotrauma 36(22):3063–3091
137. Iannucci J et al (2023) Sex-specific and traumatic brain injury effects on dopamine receptor expression in the hippocampus. Int J Mol Sci 24(22):16084
138. Xu X et al (2016) Sex-related differences in striatal dopaminergic system after traumatic brain injury. Brain Res Bull 124:214–221
139. O'Connor CA, Cernak I, Vink R (2006) The temporal profile of edema formation differs between male and female rats following diffuse traumatic brain injury. Acta Neurochir Suppl 96:121–124
140. Wright DK et al (2017) Sex matters: repetitive mild traumatic brain injury in adolescent rats. Ann Clin Transl Neurol 4(9):640–654
141. Pasam T, Dandekar MP (2023) Fecal microbiota transplantation unveils sex-specific differences in a controlled cortical impact injury mouse model. Front Microbiol 14:1336537
142. Guler HP, Zapf J, Froesch ER (1987) Short-term metabolic effects of recombinant human insulin-like growth factor I in healthy adults. N Engl J Med 317(3):137–140
143. Mukherjee S et al (2013) Increased seizure susceptibility in mice 30 days after fluid percussion injury. Front Neurol 4:28
144. D'Ambrosio R et al (2004) Post-traumatic epilepsy following fluid percussion injury in the rat. Brain 127(2):304–314
145. Kumar KM et al (2017) Male reproductive toxicity of CrVI: In-utero exposure to CrVI at the critical window of testis differentiation represses the expression of Sertoli cell tight junction proteins and hormone receptors in adult F1 progeny rats. Reprod Toxicol 69:84–98
146. Belote BL et al (2023) Applying different morphometric intestinal mucosa methods and the correlation with broilers performance under Eimeria challenge. Poult Sci 102(9):102849
147. Iannucci J, Nizamutdinov D, Shapiro LA (2022) Neurogenesis and chronic neurobehavioral outcomes are partially improved by vagus nerve stimulation in a mouse model of Gulf War illness. Neurotoxicology 90:205–215
148. Iannucci J et al (2024) Traumatic brain injury alters the effects of class II invariant peptide (CLIP) antagonism on chronic meningeal CLIP + B cells, neuropathology, and neurobehavioral impairment in 5xFAD mice. J Neuroinflammation 21(1):165
149. Bryant JD et al (2021) Neuroimmune mechanisms of cognitive impairment in a mouse model of Gulf War illness. Brain Behav Immun 97:204–218

Publisher's Note